NANO LETTERS

2001
Vol. 1, No. 12
689−692

Gold Nanoclusters Supported on MgO: Synthesis, Characterization, and Evidence of Au_6

Javier Guzman and Bruce C. Gates*

Department of Chemical Engineering and Materials Science, University of California, Davis, California 95616

Received August 15, 2001; *Revised Manuscript Received September 27, 2001*

Downloaded by NAT LIB UKRAINE on August 6, 2009
Published on October 20, 2001 on http://pubs.acs.org | doi: 10.1021/nl015605n

ABSTRACT

Gold nanoclusters on MgO powder were prepared from adsorbed $[Au(CH_3)_2(C_5H_7O_2)]$ and characterized by infrared and X-ray absorption spectroscopies. Treatment of the samples in He or H_2 at increasing temperatures removed CH_3 and $C_5H_7O_2$ ligands and caused the gold to aggregate into nanoclusters of increasing size, ultimately those with the properties of metallic gold. Treatment in He at 373 K gave clusters that are inferred to be nearly monodisperse Au_6, with first- and second-shell Au−Au coordination numbers of 4.0 ± 0.4 and 1.0 ± 0.1, respectively, corresponding to Au_6 octahedra.

Solid catalysts typically consist of nanoclusters of metal, metal oxide, or metal sulfide stably dispersed on the internal surfaces of porous supports such as metal oxides. The smallness of the nanoclusters ensures that a large fraction of the atoms in them are present at surfaces and accessible to reactants. Many important supported nanocluster catalysts are metals. Among those receiving the most attention recently is supported gold. Although gold is one of the least reactive metals, recent research has shown that gold nanoclusters on supports have surprising new catalytic properties, being active for CO oxidation at low temperatures[1−4] and selective for propene oxidation to give propene oxide.[5,6]

Supported gold has been prepared from gold salts (e.g., $HAuCl_4$[5,7]) and complexes (e.g., $Au(PPh_3)(NO_3)$[8,9]), but these precursors typically leave contaminants such as chlorine or phosphorus on the catalyst. The sizes and structures of the gold nanoclusters in these catalysts have not been determined precisely, but it has been suggested that the nanoclusters in catalysts for CO oxidation may be approximated as icosahedral and fcc cuboctahedral gold with a size distribution of 6−40 Å;[10] the presence of Au_8 clusters has also been suggested.[3,11] However, the structures are nonuniform and the structural postulates imprecise.

Our goal was to prepare and characterize supported nanoclusters of gold with a wide range of sizes and to seek preparation conditions to make them nearly monodisperse. We report the synthesis of MgO-supported gold nanoclusters formed from $[Au(CH_3)_2(acac)]$ (acac is $C_5H_7O_2$) and their characterization by extended X-ray absorption fine structure (EXAFS) spectroscopy and X-ray absorption near edge spectroscopy (XANES). $[Au(CH_3)_2(acac)]$ was chosen as the precursor because it offers the advantage of organic ligands that are readily removed under mild treatment conditions. The data show that most of the samples consist of nonuniform supported nanoclusters formed by migration and aggregation of the gold, but, with the proper choice of preparation conditions, the samples consist predominantly of supported Au_6.

Sample syntheses and transfers were performed in the absence of moisture and air with standard glovebox and vacuum line techniques. $[Au(CH_3)_2(acac)]$ (Aldrich, 98%) was brought in contact with MgO powder (EM Science, BET surface area 47 m^2/g) that had been calcined in O_2 at 673 K for 2 h followed by evacuation at 10^{-3} Torr at 673 K for 14 h. $[Au(CH_3)_2(acac)]$ was mixed with the MgO in a Schlenk flask, with the mixture composition chosen so that the resultant sample contained 1 wt % Au. Dried and deoxygenated *n*-hexane (Aldrich, 99%, dried over sodium benzophenone ketyl and deoxygenated by sparging with N_2 prior to use) was then introduced by cannula into each solid mixture in a Schlenk flask. The slurry was stirred for 1 day, and the solvent was removed by evacuation (pressure $<10^{-3}$ Torr) for 1 day.

The resultant MgO-supported sample was treated in flowing He or H_2 at atmospheric pressure as the temperature was ramped at a rate of 3 K/min from room temperature to a temperature in the range of 323−573 K to remove the ligands bonded to the gold. The treatment gas (He or H_2; Matheson, UHP grade) was purified by flow through traps containing particles of reduced Cu/Al_2O_3 and activated zeolite 4A to remove traces of O_2 and moisture, respectively.

* Corresponding author e-mail: bcgates@ucdavis.edu.

10.1021/nl015605n CCC: $20.00 © 2001 American Chemical Society
Published on Web 10/20/2001

Table 1: EXAFS Results at the Au L_{III} Edge Characterizing the Supported Species Formed by Removal of Ligands from $[Au(CH_3)_2(acac)]$ and Aggregation of the Gold on MgO after Treatment for 2 h in He or in H_2 at Various Temperatures[a]

		Au−Au first-shell contribution				Au−Au second-shell contribution			
treatment gas	treatment temp, K	N	R (Å)	$10^3 \times \Delta\sigma^2$ (Å^2)	ΔE_0 (eV)	N	R (Å)	$10^3 \times \Delta\sigma^2$ (Å^2)	ΔE_0 (eV)
none	no treatment	undetectable				undetectable			
He	323	1.1	2.92	1.12	0.45	0.5	3.95	5.32	1.23
	373	4.0	2.82	1.34	2.00	1.0	4.02	4.30	5.21
	473	9.4	2.85	5.90	4.26	3.5	4.06	5.89	11.02
	573	9.4	2.85	5.97	0.06	3.4	4.05	2.36	4.73
H_2	323	1.9	2.76	3.10	1.04	3.5	3.97	9.87	4.73
	373	7.2	2.79	8.54	1.60	3.5	3.85	8.21	9.78
	473	9.5	2.85	6.83	2.53	3.8	4.06	4.52	7.12
	573	9.4	2.85	5.97	0.06	4.0	4.05	2.36	4.73

[a] Notation: N, coordination number; R, distance between absorber and backscatterer atoms; $\Delta\sigma^2$, relative Debye−Waller factor; ΔE_0, inner potential correction. Typical errors are as follows: N, ± 10%; R, ± 0.02 Å; $\Delta\sigma^2$, ± 20%; ΔE_0, ± 20%.

Alternatively, H_2 was prepared by electrolysis of water in a Balston generator (99.99%) and then purified.

Transmission infrared (IR) spectra of the solid samples were recorded with a Bruker IFS 66v spectrometer with a spectral resolution of 4 cm^{-1}. Samples were pressed into self-supporting wafers and loaded into a cell in a drybox. The cell (In-situ Research Institute, Inc., South Bend, IN) allowed recording of spectra while the treatment gases flowed through and around the wafer at temperatures ranging from room temperature to 573 K.

X-ray absorption spectroscopy experiments were performed at beam line 2-3 of the Stanford Synchrotron Radiation Laboratory (SSRL), Stanford, California. The ring current was 50−100 mA, and the storage ring operated with an electron energy of 3 GeV. Each powder sample was loaded into an EXAFS cell,[12] which was sealed and removed from the drybox. The sample mass was chosen to give an absorbance of about 2.5 at the Au L_{III} absorption edge (11918.7 eV). Before scanning, each sample was treated in flowing He or H_2 at various temperatures for 2 h, cooled, evacuated (10^{-5} Torr), and aligned in the X-ray beam. The EXAFS data were recorded in the transmission mode after the cell had been cooled to nearly liquid nitrogen temperature. The double crystal Si(220) monochromator was detuned by 20−25% at the Au L_{III} edge to suppress higher harmonics in the X-ray beam.

EXAFS data were analyzed on the basis of experimentally and theoretically determined reference files, the former obtained from EXAFS data characterizing materials of known structure and the latter calculated by using the code FEFF 7.0.[13] Details of the preparation of reference files[14] and the analysis procedure[15,16] are presented elsewhere.

IR spectra of the samples recorded before treatment in He or H_2 include bands assigned to CH_3 (2854, 2923, 2959, and 1440 cm^{-1}) and acac (1598, 1517, and 1352 cm^{-1}).[17−19] Evidently, the precursor $[Au(CH_3)_2(acac)]$ had been adsorbed intact on the MgO. When the sample was treated in He or H_2, the CH_3 bands and the acac bands declined in intensity, disappearing when the temperature reached 573 K (Figure 1).[20]

EXAFS results characterizing the initially prepared sample (Table 1) show that there was no significant Au−Au

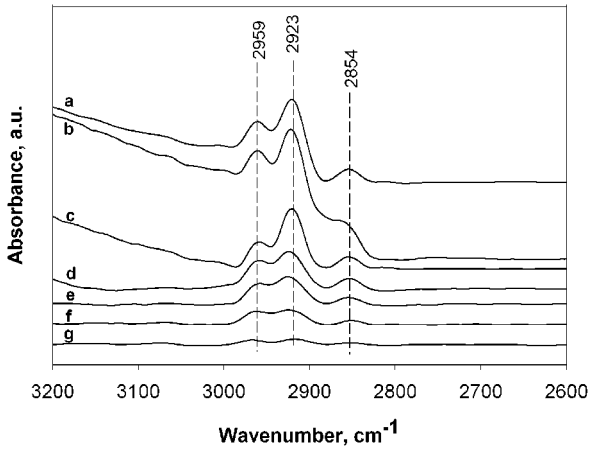

Figure 1. Infrared spectra in the ν_{CH} stretching region characterizing samples formed by deposition of $[Au(CH_3)_2(acac)]$ onto MgO and subsequent treatment under flowing He at the following temperatures (K): (a) 298, (b) 323, (c) 373, (d) 423, (e) 473, (f) 523, and (g) 573. The spectra were found to be independent of time of contact.

contribution, consistent with the presence of site-isolated mononuclear $[Au(CH_3)_2(acac)]$ on the support and negligible aggregation of the gold. However, as the samples were treated in He at increasing temperatures and the CH_3 and acac ligands removed, the Au−Au first-shell coordination number increased, indicating the formation of increasingly large gold nanoclusters (Table 1). These coordination numbers increased systematically from 1.1 to 9.4, indicating that the average number of Au atoms per nanocluster increased from about 2 to about 80, with the corresponding average nanocluster diameters being about 3 and 30 Å, respectively (Figure 2). The second-shell Au−Au coordination numbers (Table 1) range from 0.5 to 3.4, indicating three-dimensional clusters. The largest nanoclusters are characterized by an Au−Au first-shell distance of 2.85 Å, indistinguishable within the expected error from the value of 2.88 Å for bulk metallic gold.

No doubt these clusters, formed by migration and aggregation of gold on the MgO surface, are nonuniform and characterized by a range of nuclearities. However, the EXAFS data representing the sample treated in He at 373 K

Downloaded by NAT LIB UKRAINE on August 6, 2009
Published on October 20, 2001 on http://pubs.acs.org | doi: 10.1021/nl015605n

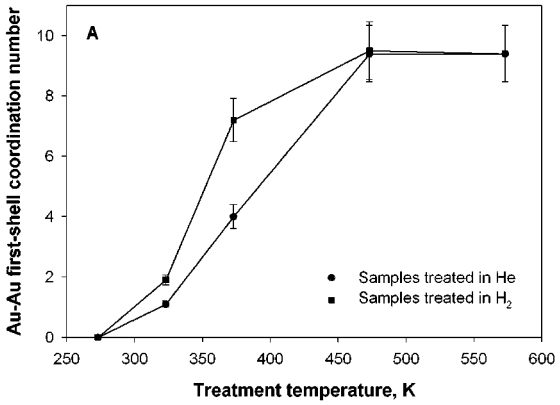

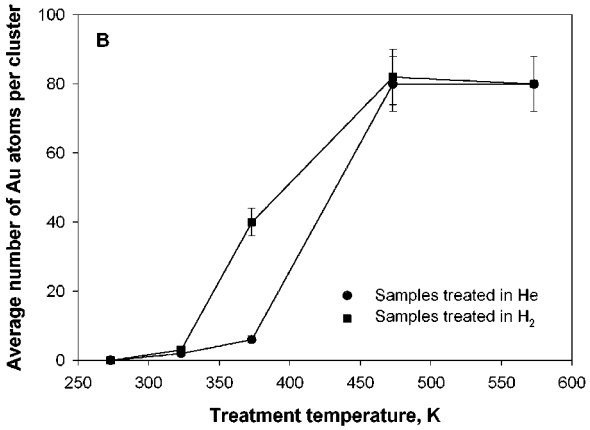

Figure 2. (A) Dependence of first-shell Au−Au coordination number of MgO-supported gold nanoclusters on preparation conditions. (B) Dependence of average nuclearity of MgO-supported gold nanoclusters on preparation conditions.

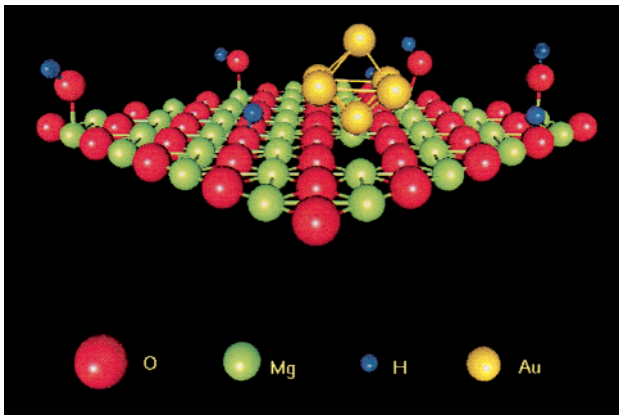

Figure 3. Schematic representation of Au_6 nanocluster supported on partially dehydroxylated MgO. Hydroxyl groups present on the support (as shown by IR spectra) are possible ligands for the gold clusters. The clusters are inferred to bond preferentially at defect sites rather than at defect-free sites, as suggested by theoretical investigations of MgO-supported osmium clusters.[22]

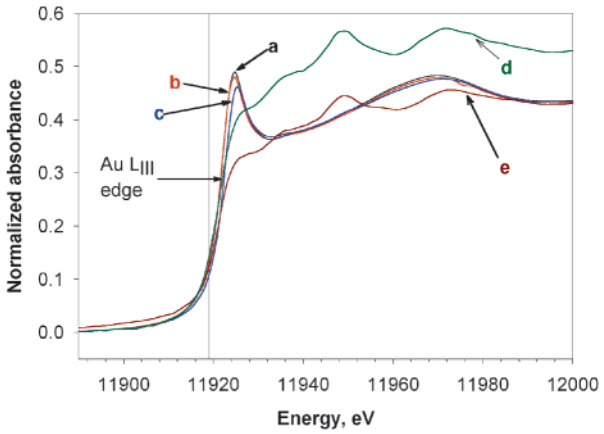

Figure 4. XANES data characterizing MgO-supported samples scanned after (a) adsorption of $[Au(CH_3)_2(acac)]$ and after subsequent exposure to He at the following temperatures (K): (b) 323, (c) 373, (d) 473, and (e) 573.

indicate a first-shell Au−Au coordination number of 4.0 (± 0.4) (with a bond distance of 2.82 ± 0.02 Å) and a second-shell Au−Au coordination number of 1.0 (± 0.1) (at a distance of 4.02 ± 0.04 Å).[21] These results point to the formation of six-atom octahedral clusters of gold (some of them ligand free, Figure 3[22]), which we suggest were nearly monodisperse and energetically favored enough to be the predominant species under these treatment conditions. Ours is the first evidence indicating the synthesis of such supported gold nanoclusters.[23−28]

When the supported precursors were treated in H_2, similar results were observed, the CH_3 and acac groups being removed as the Au−Au first-shell coordination number increased from 1.9 to 9.5 (Figure 2). The Au−Au second-shell coordination number also increased with increasing treatment temperature, the value ultimately becoming 4.0 (Table 1). The range of Au−Au coordination numbers nearly matches that resulting from He treatment, but the aggregation of the gold was initiated at lower temperatures in H_2 than in He. None of the observations of the samples treated in H_2 gave any indication of the formation of monodisperse clusters such as Au_6.

The treatments affect not only the size of the gold nanoclusters but also the electron density and the symmetry of the surroundings of gold, as shown by the XANES. The decrease in the area under the white line with increasing treatment temperature (Figure 4) indicates increasing reduction of the gold. The XANES of the largest nanoclusters essentially match that of metallic gold.[29]

In contrast, the XANES characterizing the initially prepared sample and those treated in He at 323 K and at 373 K show two peaks at energies that are 4 and 50 eV, respectively, higher than that of the X-ray absorption edge, indicating the presence of cationic gold, in agreement with the adsorption of $[Au(CH_3)_2(acac)]$ (in which the gold is a cation) intact. The disappearance of these peaks with increasing treatment temperature (Figure 4) is consistent with the conversion of cationic gold into clusters of gradually increasing size and lower oxidation state; ultimately the clusters have metallic character.[30] The samples treated in He at higher temperatures, 473 and 573 K (Figure 4), show two broad peaks, at energies 25 and 50 eV, respectively, higher than that of the edge, with the peak at 4 eV almost having disappeared; these features correspond to gold reduced to the metallic state.[31] A similar pattern was observed when the sample was treated in H_2.

Downloaded by NAT LIB UKRAINE on August 6, 2009
Published on October 20, 2001 on http://pubs.acs.org | doi: 10.1021/nl015605n

In summary, we report a new synthesis method that allows control of the average size of MgO-supported gold nanoclusters made from adsorbed [$Au(CH_3)_2$(acac)], which, upon treatment in He or H_2, is converted into gold clusters ranging in diameter from approximately 3 to 30 Å, depending on the treatment temperature. The EXAFS data are consistent with the inference that the sample prepared in He at 373 K was nearly monodisperse MgO-supported Au_6 octahedra.

Acknowledgment. This research was supported by the U.S. Department of Energy, Office of Energy Research, Office of Basic Energy Sciences, Division of Chemical Sciences, Contract FG02-87ER13790. The EXAFS experiments were done at the Stanford Synchrotron Radiation Laboratory, which is operated by Stanford University for the Department of Energy, Office of Basic Energy Sciences. The EXAFS data were analyzed with the XDAP software.[16]

References

(1) Haruta, M.; Tsubota, S.; Kobayashi, T.; Kageyama, H.; Genet, M. J.; Delmon, B. *J. Catal.* **1993**, *144*, 175.
(2) Lin, S. D.; Bollinger, M.; Vannice, M. A. *Catal. Lett.* **1993**, *17*, 245.
(3) Heiz, U.; Abbet, S.; Sanchez, A.; Schneider, W.-D.; Häkkinen, H.; Landman, U. *Phys. Chem. Clusters, Proc. Nobel Symp., 117th*, **2001**, 87.
(4) Sanchez, A.; Abbet, S.; Heiz, U.; Schneider, W.-D.; Häkkinen, H.; Barnett, R. N.; Landman, U. *J. Phys. Chem. A* **1999**, *103*, 9573.
(5) Hayashi, T.; Tanaka, K.; Haruta, M. *J. Catal.* **1998**, *178*, 566.
(6) Stangland, E. E.; Stavens, K. B.; Andres, R. P.; Delgass, W. N. *J. Catal.* **2000**, *191*, 332.
(7) Haruta, M. *Catal. Today* **1997**, *36*, 153.
(8) Kozlov, A. I.; Kozlova, A. P.; Liu, H.; Iwasawa, Y. *Appl. Catal. A* **1999**, *182*, 9.
(9) Kozlova, A. P.; Kozlov, A. I.; Sugiyama, S.; Matsui, Y.; Asakura, K.; Iwasawa, Y. *J. Catal.* **1999**, *181*, 37.
(10) Cunningham, D. A. H.; Vogel, W.; Kageyama, H.; Tsubota, S.; Haruta, M. *J. Catal.* **1998**, *177*, 1.
(11) Heiz, U.; Schneider, W.-D. *J. Phys. D* **2000**, *33*, R85.
(12) Jentoft, R. E.; Deutsch, S. E.; Gates, B. C. *Rev. Sci. Instrum.* **1996**, *67*, 2111.
(13) (a) Zabinsky, S. I.; Rehr, J. J.; Ankudinov, A.; Albers, R. C.; Eller, M. J. *Phys. Rev. B* **1995**, *52*, 2995. (b) Ankudinov, A. Ph.D. Dissertation, University of Washington, Seattle, 1996.
(14) van Zon, J. B. A. D.; Koningsberger, D. C.; van't Blik, H. F. J.; Sayers, D. E. *J. Chem. Phys.* **1985**, *82*, 5742.
(15) Kirlin, P. S.; van Zon, F. B. M.; Koningsberger, D. C.; Gates, B. C. *J. Phys. Chem.* **1990**, *94*, 8439.
(16) Vaarkamp, M.; Linders, J. C.; Koningsberger, D. C. *Phys. B* **1995**, *209*, 159.
(17) Davydov, A. A. *Infrared Spectroscopy of Adsorbed Species on the Surface of Transition Metal Oxides*; Wiley: Chichester, 1990.
(18) Harris, D. C.; Bertolucci, M. D. *Symmetry and Spectroscopy*; Oxford University Press: New York, 1978.
(19) Shimanouchi, T. *Tables of Molecular Vibrational Frequencies Consolidated Volume I*; National Bureau of Standards: Gaithersburg, MD, 1972.
(20) Samples treated at temperatures lower than 573 K still incorporated a fraction of the CH_3 and acac groups, as indicated by the IR spectra. For example, the samples treated in flowing He at 323, 373, and 473 K retained roughly 90%, 60%, and 25%, respectively, of the original organic ligands present after adsorption of [$Au(CH_3)_2$(acac)] onto MgO, as calculated from the IR spectra.
(21) Because of the noise in the low-*Z* backscatterer region, the EXAFS data provide only limited evidence of possible Au−C shells in the samples containing gold clusters from which the ligands had not been fully removed. For example, the sample treated in He at 323 K was characterized by a small Au−C shell with a coordination number of 0.5 at a distance of 1.80 Å, indicating remaining carbonaceous species, but it was not possible to fit any Au−C shells for other samples treated at temperatures below 573 K, although the IR spectra indicate the presence of organic ligands.
(22) Goellner, J. F.; Neyman, K. M.; Mayer, M.; Nörtemann, F.; Gates, B. C.; Rösch, N. *Langmuir* **2000**, *16*, 2736.
(23) The electronic structure and stability of gold nanoclusters in a vacuum have been investigated by molecular dynamics[25] and density functional theory,[27,28] the former results indicating stable three-dimensional nanoclusters of more than 4 gold atoms but the latter indicating two-dimensional nanoclusters of as many as 6 or 7 atoms (unless geometrical constraints are imposed, in which case stable octahedral structures of 6 atoms can be obtained). In view of the inconsistency of these results and the lack of theoretical investigations of the effects of supports on gold nanoclusters, an incisive comparison of our results with theoretical results awaits further work.
(24) Arslan, H.; Güven, M. H. *ARI* **1998**, *51*, 145.
(25) Erkoç, S. *Phys. E* **2000**, *8*, 210.
(26) Häberlen, O. D.; Chung, S.; Stener, M.; Rösch, N. *J. Chem. Phys.* **1997**, *106*, 5189.
(27) Häkkinen, H, Landman, U. *Phys. Rev. B* **2000**, *62*, R2287.
(28) Grönbeck, H., Andreoni, W. *Chem. Phys.* **2000**, *262*, 1.
(29) Coulthard, L.; Degen, S.; Zhu, Y.-J.; Sham, T. K. *Can. J. Chem.* **1998**, *76*, 1707.
(30) Salama, T. M.; Shido, T.; Ohnishi, R.; Ichikawa, M. *J. Phys. Chem.* **1996**, *100*, 3688.
(31) Benfield, R.; Grandjean, D.; Kröll, M.; Pugin, R.; Sawitowski, T.; Schmid, G. *J. Phys. Chem. B* **2001**, *105*, 1961.

NL015605N

Downloaded by NAT LIB UKRAINE on August 6, 2009
Published on October 20, 2001 on http://pubs.acs.org | doi: 10.1021/nl015605n